Synthesis, Spectroscopic and Structural Characterization of Mono- and Bi-nuclear Iron(III) Complexes with 2,6-Diacetylpyridine Bis(acylhydrazones)†

Alex Bonardi,[a] Curzio Merlo,[a] Corrado Pelizzi,*[,a] Giancarlo Pelizzi,[a] Pieralberto Tarasconi[a] and Fabrizio Cavatorta[b]

[a] *Istituto di Chimica Generale ed Inorganica dell'Università, Centro di Studio per la Strutturistica Diffrattometrica del C.N.R., Viale delle Scienze, I-43100 Parma, Italy*

[b] *Dipartimento di Fisica, Viale delle Scienze, I-43100 Parma, Italy*

A series of mono- and bi-nuclear iron(III) complexes with three bis(acylhydrazones) (acyl = pyridine-2-carbonyl, salicyloyl or 2-thenoyl) and the mono(2-thenoylhydrazone) of 2,6-diacetylpyridine have been prepared and characterized by IR and ^{57}Fe Mössbauer spectroscopy. The X-ray crystal structure of dichloro[2,6-diacetylpyridine bis(salicyloylhydrazonato)(4−)]bis(ethanol)diiron(III) has revealed the presence of two non-equivalent iron atoms and a tetradeprotonated and heptadentate behaviour of the hydrazone involving a bridging action of both carbonyl groups.

We have recently reported a spectroscopic and structural investigation on a series of mono- and bi-nuclear (homo and hetero) iron(II) complexes with 2,6-diacetylpyridine bis(acylhydrazones).[1] This study has confirmed the versatility these ligands show in the production of unusual stereochemistries and in the assumption of different conformations and configurations.[2,3]

The growing interest in the chemistry of binuclear metal sites and the biological importance of iron-containing systems[4–8] led us to extend our studies to complexes of iron(III) with the following 2,6-diacetylpyridine hydrazones: mono(2-thenoylhydrazone) (Hdapmt), bis(pyridine-2-carbonylhydrazone) (H_2dappc), bis(salicyloylhydrazone) (H_4daps) and bis(2-thenoylhydrazone) (H_2dapt). We use the terminology H_4daps, instead of H_2daps as previously, because, in this study we have found, for the first time, a tetradeprotonated behaviour of the ligand. The X-ray crystal structure of the complex $[Fe_2(daps)Cl_2(C_2H_5OH)_2]$ is also reported.

Experimental

Preparations.—Solvents were purified using published procedures.[9] Iron(III) chloride was commercially available (Aldrich). The hydrazones were prepared by treating 2,6-diacetylpyridine with the appropriate hydrazide as previously described.[1,2,10,11] All complexes were prepared using Fe in natural isotopic composition.

Homonuclear iron complexes. All the complexes were obtained by adding powdered anhydrous iron(III) chloride to an ethanol solution of the hydrazone (1:1 molar ratio). The solution was then refluxed for *ca.* 2 h and allowed to stand overnight. In all cases the final product was isolated in high yield (90–95%) by filtration under a nitrogen atmosphere. The compounds can also be obtained by template reactions: a mixture of 2,6-diacetylpyridine, acylhydrazine and iron(III) chloride (1:2:1 molar ratio) suspended in absolute ethanol was refluxed for 2 h.

$[Fe_2(daps)Cl_2(C_2H_5OH)_2]$. Acetic anhydride, dissolved in chloroform–acetonitrile (1:1 v/v), was added to a chloroform solution of H_4daps (2:1 molar ratio). After the addition of solid sodium acetate (CH_3CO_2Na:H_4daps $\gtrsim$ 2:1) a pale yellow precipitate was formed, which after filtration was washed with small portions of water, ethanol–water and diethyl ether (m.p. > 300 °C). From the chemical analysis the product was revealed to be the monosodium salt of H_4daps. The purified product was treated with an excess of $FeCl_2$, dissolved in absolute ethanol, for *ca.* 2 h at room temperature. A dark green crystalline product was isolated after some days by slow evaporation of the solvent (yield: *ca.* 20%).

$[Fe(H_2daps)(NCS)(OH_2)]$. An ethanolic solution of sodium thiocyanate was slowly added to an ethanolic solution of $[Fe(H_4daps)Cl_2]\cdot 0.5H_2O$ (2:1 molar ratio). The resulting solution was refluxed for *ca.* 2 h and then allowed to stand at room temperature. After slow evaporation of the solvent dark green crystals were isolated.

Measurements.—Elemental analyses for C, H, N and S were performed by Perkin-Elmer 240 automatic equipment. Determination of iron was by atomic absorption spectroscopy on a Perkin-Elmer 303-HGA 70 instrument. Mass spectra were recorded with a Varian CH-5 spectrometer at 70 eV (*ca.* 1.12×10^{-17} J). Conductance measurements (Table 1) in nitrobenzene at *ca.* 10^{-3} mol dm^{-3} were made on a Radiometer Copenhagen type CDM 38 conductivity bridge. Magnetic measurements at room temperature were carried out on a standard Gouy balance calibrated with $[Ni(en)_3][S_2O_3]$; diamagnetic corrections were applied using Pascal's constants.[12] Infrared spectra (4000–200 cm^{-1}) for KBr discs were recorded on a Perkin-Elmer 283 B spectrophotometer (cell Philips PW 9512/00), electronic spectra (900–400 nm) of methanol solutions on a JASCO 505 spectrophotometer. The ^{57}Fe absorption Mössbauer measurements were performed by using a conventional Mössbauer spectrometer working at constant acceleration, equipped with a 20 mCi ^{57}Co source in a rhodium matrix. Experiments were carried out at constant temperature keeping the absorbers in a 78–300 K cryostat. All isomeric shifts are referred to metallic iron at 298 K.

X-Ray Crystallography.—$[Fe_2(daps)Cl_2(C_2H_5OH)_2]$. All diffraction measurements were carried out at room temperature on a computer-controlled Siemens AED single-crystal diffractometer by using an irregularly shaped crystal of

† *Supplementary data available:* see **Instructions for Authors**, *J. Chem. Soc., Dalton Trans.*, 1991, **Issue 1**, **pp. xviii xxii.**

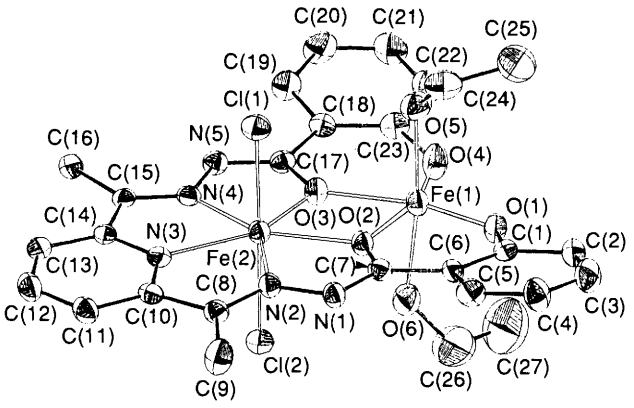

Fig. 1 ORTEP drawing of $[Fe_2(daps)Cl_2(C_2H_5OH)_2]$ with 40% probability ellipsoids

approximate dimensions 0.29 × 0.34 × 0.81 mm. The crystal system and space-group information were obtained by using peak search, centring and indexing programs and by the systematic absences (*h0l*, *l* odd and 0*k*0, *k* odd) observed during data collection.

Crystal data. $C_{27}H_{29}Cl_2Fe_2N_5O_6$, M = 702.16, monoclinic, space group $P2_1/c$, a = 19.593(4), b = 7.650(2), c = 21.418(6) Å, β = 114.73(1)°, U = 2916(1) Å^{-3}, Z = 4, D_c = 1.600 g cm^{-3}, Mo-Kα radiation (λ = 0.710 69 Å), μ(Mo-Kα) = 12.28 cm^{-1}, $F(000)$ = 1440.

Unit-cell constants, with estimated standard deviations, were determined by a least-squares fit of 28 diffractometer measured reflections distributed over a wide range of reciprocal space. The θ–2θ scan technique and niobium-filtered molybdenum radiation were used to record the intensities of 6990 reflections ($\pm h + k + l$) within the limits $2.5 < \theta < 27.0°$. After removal of space-group forbidden reflections and averaging symmetry-equivalent data, 3754 reflections with $I > 2\sigma(I)$ were considered observed and used in the refinement of the structure. There was no evidence of crystal decomposition or loss of alignment during data collection. A diffraction profile analysis was performed on all reflections using the Lehmann and Larsen algorithm.[13] The data were corrected for Lorentz and polarization factors. Corrections for absorption and extinction effects were applied during the refinement according to the empirical method of Walker and Stuart.[14]

The structure was solved by a combination of direct methods and Fourier difference techniques. The coordinates of the two independent iron atoms as well as those of the two chlorines were determined from the phasing of 344 reflections (E_{min} = 1.92) by using MULTAN 80.[15] Two subsequent difference maps yielded the positions of all remaining non-hydrogen atoms. Refinement was by full-matrix least-squares procedures based on F, minimizing the function $\Sigma w(|F_o| - |F_c|)^2$. All the hydrogen atoms of the hydrazone moiety and of one ethanol molecule were located by Fourier difference techniques as was the hydroxyl hydrogen of the second ethanol molecule, while the other five hydrogens were added in idealized positions and allowed to shift according to the movement of the parent carbon atoms. Anisotropic thermal parameters were assigned to all atoms but the hydrogens. Convergence was reached with R and R' equal to 0.0399 and 0.0574, respectively, for 481 variables refined. Complex atom-scattering factors were employed and corrections for both the real and the imaginary components were included for the non-hydrogen atoms.[16] Computations were performed on GOULD 32/77 and 6040 computers using the programs of the SHELX 76 package.[17] Other crystallographic computer programs used have been cited elsewhere.[18] Final atomic coordinates of non-hydrogen atoms are listed in Table 3, bond distances and angles in Tables 4 and 5, respectively.

Additional material available from the Cambridge Crystallographic Data Centre comprises H-atom coordinates and thermal parameters.

$[Fe(H_2daps)(NCS)(OH_2)]$. *Crystal data.* $C_{24}H_{21}FeN_6O_5S$, M = 561.37, orthorhombic, space group *Pnma*, a = 15.921(8), b = 12.454(5), c = 13.854(5) Å, U = 2747(2) Å^3, Z = 4.

Intensity data were collected out to $2\theta = 50°$ on a computer-controlled Siemens AED single-crystal diffractometer by using the θ–2θ scan technique and niobium-filtered molybdenum radiation. 2767 Reflections were collected, 1333 of which were considered observed [$I > 2\sigma(I)$].

A satisfactory refinement of the structure proved impossible owing to remarkable disorder problems. However, there is no doubt in our minds that the compound is unambiguously identified and that the basic structure consists of a seven-co-ordinate iron atom with the hydrazone molecule occupying the equatorial plane and the isothiocyanate group and one water molecule at the axial sites of a pentagonal bipyramid. Attempts to refine the structure in the space group $Pn2_1a$ and consequently to relax the symmetry were also made but were unsuccessful. The analysis of the intensity statistics clearly indicated that the cell was centrosymmetric.

Results and Discussion

All the complexes contain the hydrazone in its deprotonated form, as expected for iron(III) derivatives. It is of note that the complex $[Fe_2(daps)Cl_2(C_2H_5OH)_2]$ contains the hydrazone ligand in its tetradeprotonated form as a consequence of the experimental conditions employed. From the reaction of iron(III) chloride with H_4daps (1:1 molar ratio) two monometallic complexes with different degrees of hydration were obtained.

Owing to the poor solubility, conductivity measurements were carried out only on a limited number of samples, all of which revealed a non-electrolyte nature (Table 1).[19] The magnetic susceptibility was determined only for three complexes owing to the low amounts of the samples available and in all cases a high-spin nature was found (Table 1).[20–22]

Infrared Spectra.—A comparison between the main vibrational bands of the hydrazone in its free and co-ordinated state (Table 2) leads to the following observations: (*a*) for all the complexes the amide I band, ν(CO), undergoes a remarkable shift towards lower wave numbers [Δν = 70 (Hdapmt), 60 (H_2dapt), 55–75 (H_4daps) and 100 cm^{-1} (H_2dappc)] as a consequence of co-ordination of the carbonyl oxygen atom to the metal as well as deprotonation of the hydrazone;[23–25] (*b*) unlike the H_4daps complexes where the amide II band shifts to lower wavenumbers,[26,27] for the other complexes the amide II band exhibits a positive shift (Δν = 15–35 cm^{-1}).

The vibration at 2075 cm^{-1}, due to the stretching mode of the SCN group, is in agreement with N bonding.[27–29] Owing to the complexity of the vibrational spectrum, it is difficult to distinguish between the tetra- and bi-deprotonated character of H_4daps in $[Fe_2(daps)Cl_2(C_2H_5OH)_2]$ and in $[Fe(H_2daps)(NCS)(OH_2)]$ respectively.

X-Ray Structure of $[Fe_2(daps)Cl_2(C_2H_5OH)_2]$.—The interest in this structural study arises from several factors such as the bimetallic nature of the complex, the presence of two non-equivalent iron atoms and, as regards the hydrazone molecule, the heptadentate behaviour involving a bridging action of both carbonyl groups and the tetradeprotonated form.

The two iron atoms are both in formal oxidation state III, but have different environments, with Fe(1) six-co-ordinate and Fe(2) seven-co-ordinate (Fig. 1, Tables 3–5). The molecule as a whole comes rather close to having C_{2v} symmetry, if the ethyl groups are ignored. The co-ordination geometry around Fe(1) is severely distorted octahedral with the four hydrazone oxygens, two of which are bridging atoms, in the equatorial

Table 1 Physical and analytical data[a]

Complex	Colour	Analysis (%) C	H	N	Fe
$[Fe(dapmt)Cl_2]\cdot H_2O$[b]	Red-brown	39.0 (39.3)	3.3 (3.4)	9.8 (9.9)	13.0 (12.4)
$[Fe(dapt)Cl]\cdot 4H_2O$[b,c]	Brown	39.8 (40.0)	4.1 (4.2)	12.2 (11.8)	9.8 (9.5)
$[Fe(H_2daps)Cl]\cdot 5H_2O$[c]	Dark green	45.2 (45.4)	4.8 (5.0)	11.5 (11.4)	9.1 (8.6)
$[Fe(H_2daps)Cl]\cdot H_2O$	Red	51.3 (51.2)	3.9 (4.3)	13.0 (12.7)	10.4 (9.8)
$[Fe(H_2daps)(NCS)(OH_2)]$[b]	Dark green	51.4 (51.8)	3.8 (4.1)	15.0 (14.8)	10.0 (10.6)
$[Fe_2(daps)Cl_2(C_2H_5OH)_2]$	Dark green	46.1 (45.8)	4.4 (4.8)	10.0 (9.7)	15.9 (15.3)
$[Fe(dappc)Cl]\cdot 7H_2O$[d]	Brown	47.0 (47.2)	5.8 (5.7)	18.3 (17.9)	10.4 (9.6)
$[Fe_2(dappc)Cl_3]\cdot 3H_2O$[c]	Brown-green	60.2 (59.8)	5.5 (5.7)	23.4 (23.1)	26.6 (26.1)

[a] Calculated values are given in parentheses. [b] Sulphur analysis: $[Fe(dapmt)Cl_2]\cdot H_2O$, 7.4 (7.1); $[Fe(dapt)Cl]\cdot 4H_2O$, 11.2 (10.8), $[Fe(H_2daps)(NCS)(OH_2)]$, 5.7 (5.4%). [c] Magnetic moments, μ: $[Fe(dapt)Cl]\cdot 4H_2O$, 6.04; $[Fe(H_2daps)Cl]\cdot 5H_2O$, 5.92; $[Fe_2(dappc)Cl_3]\cdot 3H_2O$, 4.89 ($Fe^{II}$), 5.47 B.M. ($Fe^{III}$) (B.M. ≈ 9.27×10^{-24} J T^{-1}). [d] Non-electrolyte.

Table 2 Selected vibrational bands (cm^{-1})

Compound	ν(OH)	ν(NH)	Amide I	Ring	Amide II	δ(OH)	Amide III
Hdapmt	—	3155m	1690s 1645vs	1570m 1500m	1510m	—	1310vs
$[Fe(dapmt)Cl_2]\cdot H_2O$	3400w(br)	—	1575vs	—	1525s	1350m	1315m(br)
H_2dapt	—	3160m	1635vs	1565m 1500m	1510m	—	1305s
$[Fe(dapt)Cl]\cdot 4H_2O$	3420m(br)	—	1575s 1573s	—	1530s 1528s	1350s	1315m
H_4daps	3200m(br)	3290(sh)	1655vs 1640(sh)	1605m 1490mw	1555m 1550m	—	1305m
$[Fe(H_2daps)Cl]\cdot 5H_2O$	3400m(br)	—	1580m	1550m	1515s	1375vs	1330m
$[Fe(H_2daps)Cl]\cdot H_2O$	3380m(br)	—	1600vs	1565ms	1515s	1370m	1320(sh)
$[Fe(H_2daps)(NCS)(OH_2)]$	3400m(br) 3200m	—	1620(sh) 1600vs	1565m	1520ms	1370m	1305m
$[Fe_2(daps)Cl_2(C_2H_5OH)_2]$	3400m(br)	—	1620(sh) 1590s	1550ms	1490vs	1375ms 1360ms	1315m
$H_2dappc\cdot 0.5H_2O$	3460mw	3310m	1695vs	1590mw 1565mw	1510vs	—	1280m
$[Fe(dappc)Cl]\cdot 7H_2O$	3440m(br)	—	1595m	1555s 1515s	1540vs	1385s	1300m
$[Fe_2(dappc)Cl_3]\cdot 3H_2O$	3400m(br)	—	1595m	1560(sh) 1525vs	1545vs	1385vs	1305mw

Table 3 Fractional atomic coordinates ($\times 10^5$ for Fe and Cl, $\times 10^4$ for O, N and C) for $[Fe_2(daps)Cl_2(C_2H_5OH)_2]$

Atom	X/a	Y/b	Z/c	Atom	X/a	Y/b	Z/c
Fe(1)	32 121(4)	9 199(9)	51 697(3)	C(7)	2 557(2)	2 818(6)	3 773(2)
Fe(2)	14 977(3)	26 043(8)	43 977(3)	C(8)	866(2)	4 850(6)	3 136(2)
Cl(1)	10 214(7)	352(16)	37 909(6)	C(9)	805(3)	5 960(10)	2 537(3)
Cl(2)	19 746(7)	53 353(16)	50 377(7)	C(10)	266(3)	4 791(6)	3 381(2)
O(1)	3 917(2)	1 075(4)	4 799(2)	C(11)	−432(3)	5 602(7)	3 065(3)
O(2)	2 499(2)	2 263(4)	4 323(2)	C(12)	−941(3)	5 365(7)	3 344(3)
O(3)	2 227(2)	1 252(4)	5 244(2)	C(13)	−758(3)	4 341(6)	3 930(3)
O(4)	3 565(2)	−201(5)	6 018(2)	C(14)	−51(2)	3 591(6)	4 223(2)
O(5)	2 810(2)	−1 453(5)	4 677(2)	C(15)	259(2)	2 578(6)	4 871(2)
O(6)	3 493(2)	3 416(6)	5 632(2)	C(16)	−212(3)	2 115(7)	5 236(3)
N(1)	2 021(2)	3 728(5)	3 305(2)	C(17)	1 980(3)	726(6)	5 697(2)
N(2)	1 432(2)	3 876(5)	3 494(2)	C(18)	2 462(3)	−406(6)	6 256(2)
N(3)	440(2)	3 837(5)	3 947(2)	C(19)	2 155(3)	−1 165(7)	6 675(3)
N(4)	943(2)	2 129(5)	5 053(2)	C(20)	2 553(3)	−2 297(8)	7 190(3)
N(5)	1 315(2)	1 161(5)	5 641(2)	C(21)	3 282(3)	−2 705(8)	7 313(3)
C(1)	3 869(3)	1 579(6)	4 190(2)	C(22)	3 593(3)	−1 988(8)	6 912(3)
C(2)	4 488(3)	1 219(7)	4 040(3)	C(23)	3 206(3)	−837(7)	6 378(2)
C(3)	4 486(3)	1 699(8)	3 424(3)	C(24)	2 827(4)	−2 133(8)	4 062(4)
C(4)	3 875(3)	2 488(8)	2 928(3)	C(25)	3 536(5)	−3 107(11)	4 207(5)
C(5)	3 266(3)	2 839(7)	3 048(3)	C(26)	4 170(5)	4 288(12)	5 946(5)
C(6)	3 237(2)	2 408(6)	3 673(2)	C(27)	4 773(5)	3 469(13)	6 400(5)

plane and the oxygen atoms of the two ethanol molecules in the axial positions. Strong distortion of the octahedral environment is seen in the departure from 180° of the angles O(1)–Fe(1)–O(3) 158.4(2)° and O(2)–Fe(1)–O(4) 159.2(2)°, and from 90° of O(1)–Fe(1)–O(4) 114.0(2)° and O(2)–Fe(1)–O(3) 71.7(1)°. Other angles in the co-ordination sphere are considerably closer to those expected for an idealized geometry as can be seen from the values given in Table 5. The Fe–O distances to the oxygens of ethanol, 2.082(5) and 2.115(5) Å, lie at the lower limit of the rather narrow range, 2.113(8)–2.160(8) Å, covered by the very

few examples of iron(III)–ethanol bonds reported to date.[30–32] Atom Fe(2) lies in a slightly distorted pentagonal-bipyramidal environment where the two bridging oxygens and three nitrogens from the hydrazone molecule form the equatorial ligand set and the two chlorine atoms, one of which is more weakly bound, are the apical ligands. Bond angles around Fe(2) show only small departures from the ideal pentagonal-bipyramidal values (Table 5). The N_3O_2 equatorial donor set of atoms are coplanar to within 0.01 Å. The apical chlorine donors are perpendicular to the equatorial plane [89.11(6)°]. The co-ordination polyhedron and donor atoms are the same as in the structures of dichloro[2,6-diacetylpyridine bis(semicarbazone)]iron(III) chloride dihydrate[33] and dichloro[2,6-diacetylpyridine bis(salicyloylhydrazone)]iron(II) monohydrate hemitoluene.[1] These compounds differ from the one reported here in having a monometallic nature. The hydrazone ligand uses seven of its nine potential donors in co-ordination to the two metal atoms. Nevertheless, the bonds it makes are nine, as it interestingly functions as a bridge through the two carbonyl oxygens linking the two iron atoms to give a dinuclear structure. To our knowledge, this represents the first known example of an acylhydrazone metal complex with such a type of bridging. Moreover, this is the first case where H_4daps has been found to be tetradeprotonated. Common features to the four complexes of the same ligand previously characterized by X-ray diffraction, namely $SnPr_2(H_2daps)$,[11] $[Ni(H_4daps)(OH_2)_2][NO_3]_2 \cdot 1.5H_2O$,[34] $[Cd(H_4daps)Cl_2] \cdot CHCl_3 \cdot CH_3OH$,[3] and $[Fe(H_4daps)Cl_2] \cdot H_2O \cdot 0.5C_6H_5CH_3$[1] are the monometallic nature, the pentagonal-bipyramidal metal environment and the quinquedentate N_3O_2 ligand behaviour of H_4daps. The main difference among these structures concerns the acid properties of the ligand which is bideprotonated in the tin derivative and remains neutral in the other three.

The bridging Fe(1)O(2)Fe(2)O(3) atoms are coplanar within experimental error and form a rhombus with acute vertex angles at iron, 71.7(1) and 70.8(1)°, obtuse at oxygen, 108.4(1) and 109.2(2)°. As a consequence, inside the rhombus the two O atoms approach relatively close to each other, 2.378(5) Å, while the two Fe atoms become more distant, at 3.321(1) Å. Besides this four-membered ring, there are six other chelate rings in the structure. The two rings around Fe(1) are both six-membered with maximum deviations from planarity of 0.08 and 0.12 Å, respectively. The mode of distortion is the same in the two rings, with the two oxygens and the carbon bound to the bridging oxygen at the opposite side with respect to the other two carbons. The four chelate rings around Fe(2) are all five-membered. Least-squares planes drawn through the individual rings show that in each of them the five constituent atoms are very nearly coplanar, the deviations from the corresponding least-squares plane being 0.05 Å or less.

A further point of interest is that the hydrazone, as a whole, can be considered, even if only roughly, approximately planar, the largest deviation of atoms from the plane of best fit being 0.4 Å. A different situation has been observed in the only other structurally characterized hydrazone complex with a 2:1 metal:ligand ratio,[35] where the ligand is fully non-planar, the side chains being twisted by considerably large amounts out of the plane of the central pyridine ring. On the contrary, a rather high degree of planarity of the hydrazone ligand seems to be,

Table 4 Bond distances (Å) for $[Fe_2(daps)Cl_2(C_2H_5OH)_2]$

Fe(1)–O(1)	1.862(4)	N(5)–C(17)	1.302(7)
Fe(1)–O(2)	2.044(3)	C(1)–C(2)	1.406(9)
Fe(1)–O(3)	2.019(4)	C(1)–C(6)	1.418(6)
Fe(1)–O(4)	1.861(4)	C(2)–C(3)	1.368(10)
Fe(1)–O(5)	2.082(5)	C(3)–C(4)	1.365(8)
Fe(1)–O(6)	2.115(5)	C(4)–C(5)	1.348(10)
Fe(2)–Cl(1)	2.326(1)	C(5)–C(6)	1.403(9)
Fe(2)–Cl(2)	2.459(1)	C(6)–C(7)	1.468(8)
Fe(2)–O(2)	2.051(4)	C(8)–C(9)	1.501(9)
Fe(2)–O(3)	2.057(3)	C(8)–C(10)	1.473(8)
Fe(2)–N(2)	2.122(4)	C(10)–C(11)	1.393(6)
Fe(2)–N(3)	2.107(4)	C(11)–C(12)	1.373(9)
Fe(2)–N(4)	2.135(5)	C(12)–C(13)	1.392(8)
O(1)–C(1)	1.326(7)	C(13)–C(14)	1.385(6)
O(2)–C(7)	1.302(6)	C(14)–C(15)	1.480(6)
O(3)–C(17)	1.315(7)	C(15)–C(16)	1.479(9)
O(4)–C(23)	1.334(7)	C(17)–C(18)	1.459(6)
O(5)–C(24)	1.430(9)	C(18)–C(19)	1.399(9)
O(6)–C(26)	1.383(10)	C(18)–C(23)	1.409(7)
N(1)–N(2)	1.379(7)	C(19)–C(20)	1.362(8)
N(1)–C(7)	1.308(5)	C(20)–C(21)	1.375(9)
N(2)–C(8)	1.288(5)	C(21)–C(22)	1.360(10)
N(3)–C(10)	1.332(6)	C(22)–C(23)	1.390(7)
N(3)–C(14)	1.337(7)	C(24)–C(25)	1.489(12)
N(4)–N(5)	1.378(5)	C(26)–C(27)	1.331(12)
N(4)–C(15)	1.276(6)		

Table 5 Bond angles (°) for $[Fe_2(daps)Cl_2(C_2H_5OH)_2]$

O(1)–Fe(1)–O(2)	86.7(1)	Cl(2)–Fe(2)–N(4)	87.6(1)	Fe(2)–N(3)–C(14)	119.1(3)	N(3)–C(10)–C(11)	120.7(5)
O(1)–Fe(1)–O(3)	158.4(2)	O(2)–Fe(2)–O(3)	70.8(1)	Fe(2)–N(3)–C(10)	119.4(4)	C(10)–C(11)–C(12)	118.4(5)
O(1)–Fe(1)–O(4)	114.0(2)	O(2)–Fe(2)–N(2)	71.5(1)	C(10)–N(3)–C(14)	121.5(4)	C(11)–C(12)–C(13)	120.4(5)
O(1)–Fe(1)–O(5)	91.7(2)	O(2)–Fe(2)–N(3)	144.1(1)	Fe(2)–N(4)–C(15)	120.8(3)	C(12)–C(13)–C(14)	118.3(5)
O(1)–Fe(1)–O(6)	92.8(2)	O(2)–Fe(2)–N(4)	142.8(1)	Fe(2)–N(4)–N(5)	118.2(3)	N(3)–C(14)–C(13)	120.7(4)
O(2)–Fe(1)–O(3)	71.7(1)	O(3)–Fe(2)–N(2)	142.2(2)	N(5)–N(4)–C(15)	120.6(4)	C(13)–C(14)–C(15)	125.6(5)
O(2)–Fe(1)–O(4)	159.2(2)	O(3)–Fe(2)–N(3)	144.7(2)	N(4)–N(5)–C(17)	110.3(4)	N(3)–C(14)–C(15)	113.6(4)
O(2)–Fe(1)–O(5)	90.9(2)	O(3)–Fe(2)–N(4)	72.1(1)	O(1)–C(1)–C(6)	125.2(5)	N(4)–C(15)–C(14)	113.2(4)
O(2)–Fe(1)–O(6)	84.8(2)	N(2)–Fe(2)–N(3)	72.8(2)	O(1)–C(1)–C(2)	117.1(4)	C(14)–C(15)–C(16)	121.2(5)
O(3)–Fe(1)–O(4)	87.6(2)	N(2)–Fe(2)–N(4)	145.5(2)	C(2)–C(1)–C(6)	117.7(5)	N(4)–C(15)–C(16)	125.6(5)
O(3)–Fe(1)–O(5)	88.8(2)	N(3)–Fe(2)–N(4)	72.8(2)	C(1)–C(2)–C(3)	120.8(6)	O(3)–C(17)–N(5)	121.1(4)
O(3)–Fe(1)–O(6)	85.4(2)	Fe(1)–O(1)–C(1)	132.7(3)	C(2)–C(3)–C(4)	121.1(6)	N(5)–C(17)–C(18)	120.5(5)
O(4)–Fe(1)–O(5)	90.0(2)	Fe(1)–O(2)–Fe(2)	108.4(1)	C(3)–C(4)–C(5)	119.9(6)	O(3)–C(17)–C(18)	118.4(4)
O(4)–Fe(1)–O(6)	92.4(2)	Fe(2)–O(2)–C(7)	118.6(3)	C(4)–C(5)–C(6)	121.8(6)	C(17)–C(18)–C(19)	117.9(4)
O(5)–Fe(1)–O(6)	173.6(2)	Fe(1)–O(2)–C(7)	132.9(3)	C(1)–C(6)–C(5)	118.7(5)	C(17)–C(18)–C(23)	123.7(4)
Cl(1)–Fe(2)–Cl(2)	178.78(7)	Fe(1)–O(3)–Fe(2)	109.2(2)	C(5)–C(6)–C(7)	119.3(5)	C(19)–C(18)–C(23)	118.3(4)
Cl(1)–Fe(2)–O(2)	91.3(1)	Fe(2)–O(3)–C(17)	118.1(3)	C(1)–C(6)–C(7)	122.1(4)	C(18)–C(19)–C(20)	121.9(6)
Cl(1)–Fe(2)–O(3)	92.1(1)	Fe(1)–O(3)–C(17)	132.7(3)	N(1)–C(7)–C(6)	119.3(4)	C(19)–C(20)–C(21)	119.8(6)
Cl(1)–Fe(2)–N(2)	91.2(1)	Fe(1)–O(4)–C(23)	131.5(4)	O(2)–C(7)–C(6)	119.4(4)	C(20)–C(21)–C(22)	119.4(6)
Cl(1)–Fe(2)–N(3)	92.0(1)	Fe(1)–O(5)–C(24)	129.4(4)	O(2)–C(7)–N(1)	121.3(5)	C(21)–C(22)–C(23)	122.7(6)
Cl(1)–Fe(2)–N(4)	91.6(1)	Fe(1)–O(6)–C(26)	132.2(5)	N(2)–C(8)–C(10)	112.8(4)	C(18)–C(23)–C(22)	117.8(5)
Cl(2)–Fe(2)–O(2)	89.9(1)	N(2)–N(1)–C(7)	108.8(4)	N(2)–C(8)–C(9)	125.2(5)	O(4)–C(23)–C(22)	117.9(5)
Cl(2)–Fe(2)–O(3)	88.5(1)	Fe(2)–N(2)–N(1)	119.4(3)	C(9)–C(8)–C(10)	122.0(5)	O(4)–C(23)–C(18)	124.2(4)
Cl(2)–Fe(2)–N(2)	89.0(1)	N(1)–N(2)–C(8)	119.4(4)	N(3)–C(10)–C(8)	113.7(4)	O(5)–C(24)–C(25)	111.7(6)
Cl(2)–Fe(2)–N(3)	87.0(1)	Fe(2)–N(2)–C(8)	121.1(3)	C(8)–C(10)–C(11)	125.6(4)	O(6)–C(26)–C(27)	120.4(9)

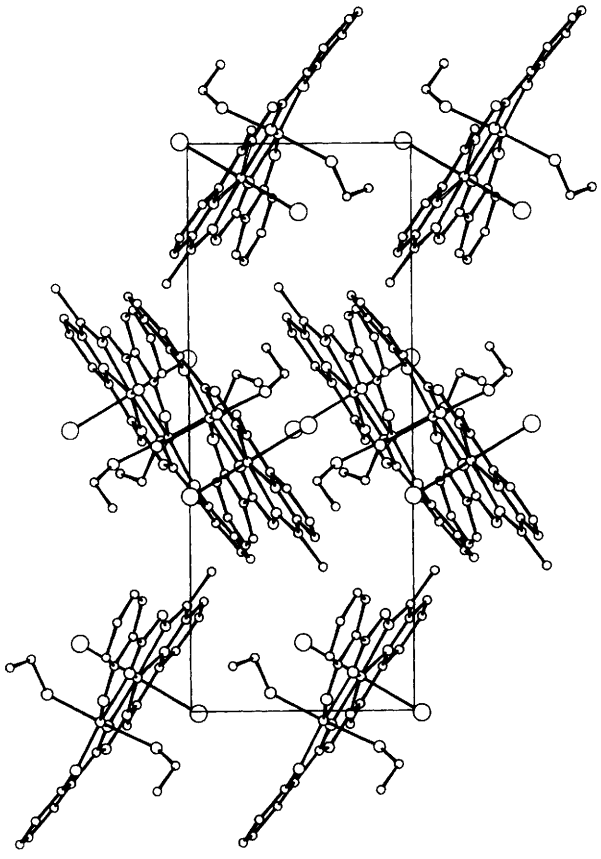

Fig. 2 Packing diagram of $[Fe_2(daps)Cl_2(C_2H_5OH)_2]$ viewed down the *a* axis

Table 6 Mössbauer data[a] ($mm\ s^{-1}$)

Compound		T/K	δ[b]	ΔE_Q	I[c]
1	$[Fe(dappc)Cl]\cdot 7H_2O$	300	0.372(5)	0.452(6)	0.601(8)
1b	$[Fe(dappc)Cl]\cdot 7H_2O$	78	0.456(3)	0.298(3)	0.611(5)
2	$[Fe(H_2daps)Cl]\cdot 5H_2O$	300	0.659(6)	0.40(1)	0.66(1)
3	$[Fe(dapmt)Cl_2]\cdot H_2O$	300	0.65(1)	0.54(1)	0.41(1)
4	$[Fe(dapt)Cl]\cdot 4H_2O$	300	0.769(6)	0.510(5)	0.56(1)
5	$[Fe_2(dappc)Cl_3]\cdot 3H_2O$	300	0.288(8)	0.500(5)	0.41(3)[d]
			0.528(8)	0.639(6)	0.29(3)
6	$[Fe_2(daps)Cl_2(C_2H_5OH)_2]$	300	0.459(2)	1.063(2)	0.191(2)[e]
			0.494(2)	2.076(2)	0.195(2)

[a] Errors affecting the last figure reported in parentheses. [b] Relative to natural Fe foil. [c] Linewidth at half maximum. [d] Percentage of the total area covered from components of the doublet at lower δ: 49.3(8)%. [e] Percentage of the total area covered from components of the external doublet: 50.2(4)%.

with only one exception,[2] a peculiarity of all metal complexes having a 1:1 metal:ligand ratio.

Consistent with the significant difference in the two Fe–Cl bond lengths, Fe(2)–Cl(1) 2.326(1) and Fe(2)–Cl(2) 2.459(1) Å, Cl(1) does not enter into the hydrogen-bonding scheme, whereas Cl(2) forms two hydrogen bonds to the hydroxyl oxygens of the two ethanol groups: one, intramolecular, being internally hydrogen bonded to O(6) [Cl(2) ··· O(6) 3.075(4) Å, Cl(2) ··· H–O(6) 164°] and the other, intermolecular, involving the O(5) atom of an adjacent ethanol molecule [Cl(2) ··· O(5) ($x, y + 1, z$) 3.220(5) Å, Cl(2) ··· H–O(5) 131°]. There are only two van der Waals contacts less than 3.4 Å, *i.e.* C(13) ··· C(15^{I}) 3.318(7) and N(5) ··· C(16^{II}) 3.329(6) Å, where I is $\bar{x}$, $1 - y$, $1 - z$ and II $\bar{x}, \bar{y}, 1 - z$. The packing of the molecules is shown in Figs. 2 and 3.

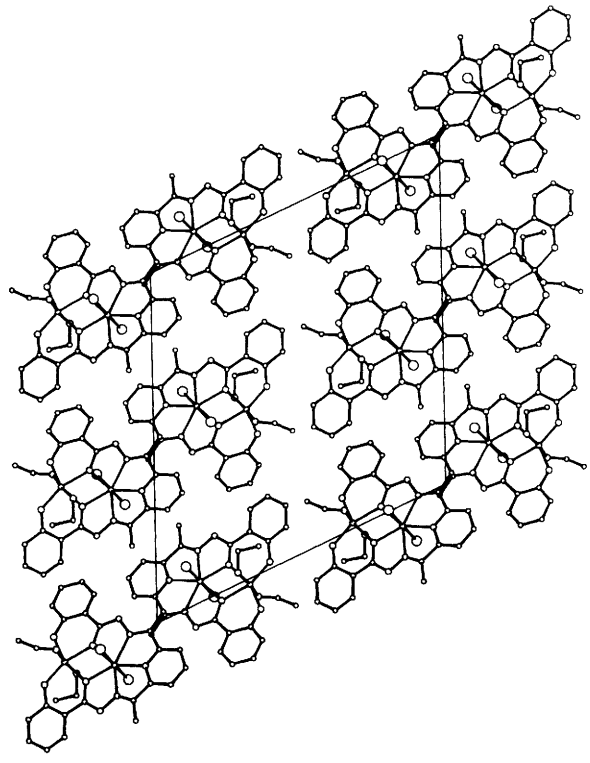

Fig. 3 Packing diagram of $[Fe_2(daps)Cl_2(C_2H_5OH)_2]$ viewed down the *b* axis

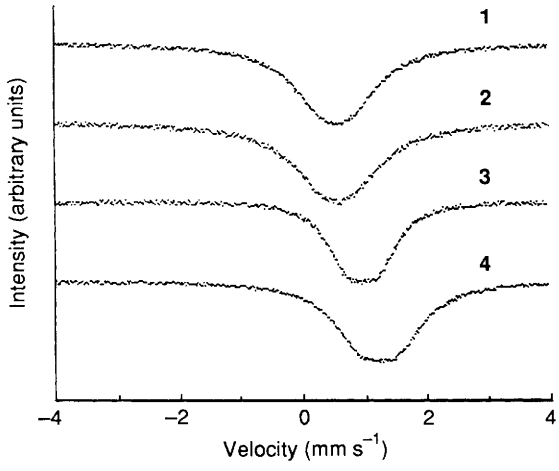

Fig. 4 Mössbauer spectra of mononuclear iron compounds at room temperature: $[Fe(dappc)Cl]\cdot 7H_2O$ **1**; $[Fe(H_2daps)Cl]\cdot 5H_2O$ **2**; $[Fe(dapmt)Cl_2]\cdot H_2O$ **3**; $[Fe(dapt)Cl]\cdot 4H_2O$ **4** (numbers refer to Table 6)

^{57}Fe *Mössbauer Spectra.*—The compounds which have been examined are listed in Table 6 together with the results from the best-fitting procedure. The experimental spectra have been fitted using a program based on a gradient algorithm to minimize the χ^2, with the possibility to choose between different line shapes.

In contrast to the case of iron(II) complexes,[1] for the present compounds no apparent asymmetry in the intensity of the doublet components was observed. Therefore, the fitting was straightforward using a single symmetric doublet for all monometallic complexes and two symmetric doublets for $[Fe_2(daps)Cl_2(C_2H_5OH)_2]$ and $[Fe_2(dappc)Cl_3]\cdot 3H_2O$. In all cases the best χ^2 was obtained when the fitting was performed using Lorentzian line shapes.

In the case of monometallic compounds (Fig. 4), the isomer shift δ and the quadrupole splitting ΔE_Q are consistent with

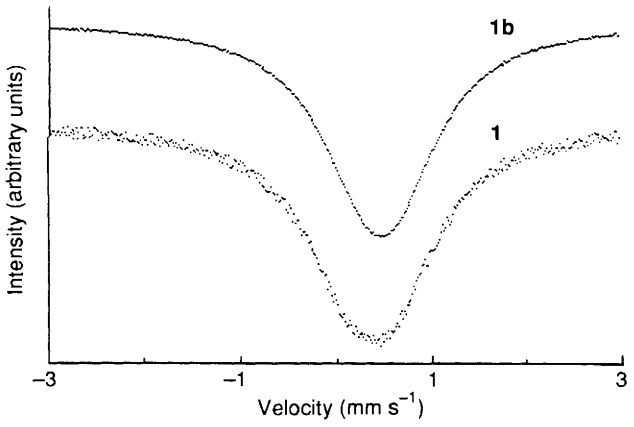

Fig. 5 Mössbauer spectra of [Fe(dappc)Cl]·7H_2O at room (**1**) and at liquid-nitrogen (**1b**) temperature (numbers refer to Table 6)

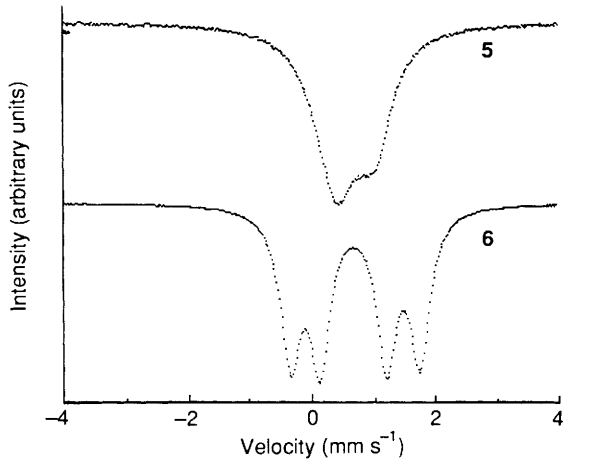

Fig. 6 Mössbauer spectra at room temperature of [Fe_2(dappc)Cl_3]·3H_2O **5** and [Fe_2(daps)Cl_2(C_2H_5OH)$_2$] **6** (numbers refer to Table 6)

high-spin Fe^{3+} even if a δ value as high as 0.77 mm s^{-1} obtained for [Fe(dapt)Cl]·4H_2O is relatively uncommon. It is interesting that the isomer shift increases on going from H_2dappc to H_4daps and to H_2dapt as with the analogous iron(II) compounds. There is probably a systematic increase in d-electron density on the iron atom in this sequence of ligands.

We have measured the spectrum of [Fe(dappc)Cl]·7H_2O both at 300 and at 78 K (Fig. 5). Temperature reduction induces a substantial increase in δ and a sensible decrement in quadrupole splitting, while the linewidth is almost unaffected. Such modifications were not observed in similar compounds [36] and are not explained by the usual models for the temperature dependence of Mössbauer parameters. Further investigations are then required to understand this behaviour which does not appear to be related to some temperature-induced structural rearrangement.

We have recorded the spectra for two binuclear iron complexes: [Fe_2(dappc)Cl_3]·3H_2O and [Fe_2(daps)Cl_2(C_2H_5OH)$_2$] (Fig. 6). In the case of [Fe_2(dappc)Cl_3]·3H_2O the Mössbauer parameters leave some uncertainty in the assignment of the electronic configuration of one of the iron atoms: one atom exhibits a typical high-spin Fe^{3+} configuration (δ = 0.288, ΔE_Q = 0.500 mm s^{-1}), while it is difficult to define clearly the state of the other (δ = 0.528, ΔE_Q = 0.639 mm s^{-1}).

The complex [Fe_2(daps)Cl_2(C_2H_5OH)$_2$] presents a structured spectrum formed by two symmetric and well separated narrow doublets. While δ values confirm the Fe^{3+} configuration, high spin is not clearly demonstrated by the high values of the quadrupole splitting. In view of the unusual stereochemistry of this compound and of the high anisotropy of the iron sites, we still believe that a high-spin configuration is the most probable one. It is also of note how the different values for ΔE_Q confirm the difference in the local symmetry for the two iron sites found in the structure.

A certain line broadening is common to all of these compounds. One reason for this behaviour could be the presence of a different packing of the molecules in the microcrystals leading to small distortions of the iron surroundings with a consequent smearing of the quadrupole doublet. A noticeable exception is the case of [Fe_2(daps)Cl_2-(C_2H_5OH)$_2$], where particularly sharp lines have been observed; in this case the narrowing of the lines is probably due to an increased uniformity of the sites associated to a stronger lattice coupling.

Acknowledgements

The financial support of the Ministero della Pubblica Istruzione (40%) is gratefully acknowledged. We thank Mr. Andrea Cantoni and Mr. Gianfranco Pasquinelli for their valuable technical assistance.

References

1 A. Bonardi, C. Carini, C. Merlo, C. Pelizzi, G. Pelizzi, P. Tarasconi, F. Vitali and F. Cavatorta, *J. Chem. Soc., Dalton Trans.*, 1990, 2771.
2 C. Lorenzini, C. Pelizzi, G. Pelizzi and G. Predieri, *J. Chem. Soc., Dalton Trans.*, 1983, 2155.
3 C. Pelizzi, G. Pelizzi and F. Vitali, *J. Chem. Soc., Dalton Trans.*, 1987, 177.
4 S. A. Cotton, *Coord. Chem. Rev.*, 1972, **8**, 185.
5 J. P. Collman, R. R. Gagne, C. A. Reed, T. R. Halbert, G. Lang and W. T. Robinson, *J. Am. Chem. Soc.*, 1975, **97**, 1427.
6 R. H. Petty, B. R. Welch, L. J. Wilson, L. A. Bottomley and K. M. Kadish, *J. Am. Chem. Soc.*, 1980, **102**, 611.
7 J. P. Collman and S. E. Groh, *J. Am. Chem. Soc.*, 1982, **104**, 1391.
8 T. B. Murphy, N. J. Rose, V. Schomaker and A. Aruffo, *Inorg. Chim. Acta*, 1985, **108**, 183.
9 D. D. Perrin, W. L. F. Armarego and D. R. Perrin, *Purification of Laboratory Chemicals*, Pergamon, Oxford, 1966.
10 C. Pelizzi and G. Pelizzi, *Acta Crystallogr., Sect. B*, 1979, **35**, 126.
11 C. Pelizzi and G. Pelizzi, *J. Chem. Soc., Dalton Trans.*, 1980, 1970.
12 *Modern Coordination Chemistry*, eds. J. Lewis and R. G. Williams, Interscience, New York, 1964.
13 M. S. Lehmann and F. K. Larsen, *Acta Crystallogr., Sect. A*, 1974, **30**, 580.
14 N. Walker and D. Stuart, *Acta Crystallogr., Sect. A*, 1983, **39**, 158.
15 P. Main, MULTAN 80, A system of computer programs for the automatic solution of crystal structures from X-ray diffraction data, University of York, 1980.
16 *International Tables for X-Ray Crystallography*, Kynoch Press, Birmingham, 1974, vol. 4.
17 G. M. Sheldrick, SHELX 76, Program for Crystal Structure Determination, University of Cambridge, 1976.
18 D. Delledonne, G. Pelizzi and C. Pelizzi, *Acta Crystallogr., Sect. C*, 1987, **43**, 1502.
19 W. J. Geary, *Coord. Chem. Rev.*, 1971, **7**, 81.
20 S. M. Nelson and D. H. Busch, *Inorg. Chem.*, 1969, **8**, 1859.
21 M. G. B. Drew, A. Hamid bin Othman, P. D. A. McIlroy and S. M. Nelson, *J. Chem. Soc., Dalton Trans.*, 1975, 2507.
22 J. C. Fanning, J. L. Resce, G. C. Lickfield and M. E. Kotun, *Inorg. Chem.*, 1985, **24**, 2884.
23 M. F. Iskander and S. Saddeck, *Inorg. Chim. Acta*, 1977, **22**, 141.
24 C. Hershko, S. Avramovici Grisarn, G. Link, L. Gelfand and S. Sarel, *J. Lab. Clin. Med.*, 1981, **98**, 99.
25 O. P. Pandey, *Polyhedron*, 1987, **6**, 1021.
26 K. K. Narang and A. Aggarwal, *Inorg. Chim. Acta*, 1974, **9**, 137.
27 A. Ghany, M. Al-Daher and K. W. Bagnall, *J. Chem. Soc., Dalton Trans.*, 1986, 843.
28 A. Lavery, S. M. Nelson and M. G. B. Drew, *J. Chem. Soc., Dalton Trans.*, 1987, 2975.
29 E. Bouwman, W. L. Driessen and J. Reedijk, *J. Chem. Soc., Dalton Trans.*, 1988, 1337.
30 F. W. B. Einstein and A. C. Willis, *Inorg. Chem.*, 1978, **17**, 3040.
31 J. A. Bertrand, E. Fujita, P. G. Eller and D. G. van Der veer, *Inorg. Chem.*, 1978, **17**, 3571.

32 P. Gans, G. Buisson, E. Duee, J.-R. Regnard and J.-C. Marchon, *J. Chem. Soc., Chem. Commun.*, 1979, 393.
33 G. J. Palenik, D. W. Wester, U. Rychlewska and R. C. Palenik, *Inorg. Chem.*, 1976, **15**, 1814.
34 C. Pelizzi, G. Pelizzi, S. Porretta and F. Vitali, *Acta Crystallogr., Sect. C*, 1986, **42**, 1131.
35 A. Mangia, C. Pelizzi and G. Pelizzi, *Acta Crystallogr., Sect. B*, 1974, **30**, 2146.
36 M. Mohan and M. Kumar, *Polyhedron*, 1985, **4**, 1929.

Received 17*th July* 1990; *Paper* 0/03213A